On the accuracy of the rotation form in simulations of the Navier–Stokes equations

William Layton [a],[*],[1], Carolina C. Manica [b], Monika Neda [c], Maxim Olshanskii [d],[2], Leo G. Rebholz [e]

[a] Department of Mathematics, University of Pittsburgh, United States
[b] Departamento de Matemática Pura e Aplicada, Universidade Federal do Rio Grande do Sul, Brazil
[c] Department of Mathematical Sciences, University of Nevada, Las Vegas, United States
[d] Department of Mechanics and Mathematics, Moscow State M. V. Lomonosov University, Moscow 119899, Russia
[e] Department of Mathematical Sciences, Clemson University, United States

ARTICLE INFO

ABSTRACT

The rotation form of the Navier–Stokes equations nonlinearity is commonly used in high Reynolds number flow simulations. It was pointed out by a few authors (and not widely known apparently) that it can also lead to a less accurate approximate solution than the usual $\mathbf{u} \cdot \nabla \mathbf{u}$ form. We give a different explanation of this effect related to (i) resolution of the Bernoulli pressure, and (ii) the scaling of the coupling between velocity and pressure error with respect to the Reynolds number. We show analytically that (i) the difference between the two nonlinearities is governed by the difference in the resolution of the Bernoulli and kinematic pressures, and (ii) a simple, linear grad–div stabilization ameliorates much of the bad scaling of the velocity error with respect to Re. The rotation form does have superior conservation properties to the alternatives and it appears to be amenable to more efficient preconditioners. Thus, the rotational form with grad–div stabilization is a promising method. We also give experiments that show bad velocity approximation is tied to poor pressure resolution in either form.

© 2009 Elsevier Inc. All rights reserved.

1. Introduction

The nonlinearity in the Navier–Stokes equations (NSE) can be written in several ways, which, while equivalent for the continuous NSE, lead to discretizations with different algorithmic costs, conserved quantities, and approximation accuracy, e.g. [9,10]. These forms include the convective form, the skew-symmetric form and the rotation form, given respectively by

$$\mathbf{u} \cdot \nabla \mathbf{u}, \quad \mathbf{u} \cdot \nabla \mathbf{u} + \frac{1}{2}(\operatorname{div}\mathbf{u})\mathbf{u}, \quad \text{and} \quad (\nabla \times \mathbf{u}) \times \mathbf{u}.$$

In turbulent flow simulations, different forms of the nonlinearity are used for different reasons. The algorithmic advantages and superior conservation properties of the rotation form (summarized in Section 2.2) have led to it being a very common

---

choice, see, e.g. Chapter 7 in [5,6,24]. Herein we reveal potential limitations of rotation form, and suggest a way to overcome them.

It is known from Horiuti [14], Horiuti and Itami [15] and Zang [33] that the rotation form can lead to a less accurate approximate solution when discretized by commonly used numerical methods. Horiuti [14] and Zang [33] each give numerical experiments and accompanying analytic arguments suggesting that the accuracy loss may happen due, respectively, to discretization errors in the near wall regions (Horiuti, for finite-difference methods) and to greater aliasing errors (Zang, for spectral methods). We have noticed the same loss of accuracy in experiments from [20,26] (for finite element methods) and suggest herein a third possibility that it is due to a combination of:

1. The Bernoulli or dynamic pressure $P = p + \frac{1}{2}|\mathbf{u}|^2$ is generically much more complex than the pressure p, and thus
2. Meshes upon which p is fully resolved are typically under resolved for P, and
3. As the Reynolds number increases, the discrete momentum equation with either form of the nonlinearity magnifies the pressure error's effect upon the velocity error.

We will see, for example, that in the usual formulation *Velocity Error $\sim Re^*$ Pressure Error*, (2.13). Thus, interestingly, some of the loss of accuracy, although triggered by the nonlinear term, is due to connections between variables already present in the linear Stokes problem.

In finite element methods (FEM) the inf–sup condition for stability of the pressure places a strong condition linking velocity and pressure degrees of freedom. This condition, while quite technical when precisely stated, roughly implies that for lower order approximations the pressure degrees of freedom should correspond to the velocity degrees of freedom on a mesh one step coarser than the velocity mesh, while for higher order finite elements the polynomial degree of pressure approximations is less than the polynomial degree of velocity approximations. Thus, in either case for velocities $\mathbf{u}$ and Bernoulli pressures P with the same complex structures, as the mesh is refined the velocity will be often fully resolved before the Bernoulli pressure is well-resolved, see the experiments in Section 3.3 involving flow around a cylinder. Further, when an artificial problem, constructed so the kinematic pressure and Bernoulli pressure reverse complexity, is solved the observed error behavior is reversed: the convective form has much greater error than the rotation form, Section 3.2.

The question of resolution is reminiscent of Horiuti's argument based on truncation errors in boundary layers. For example, even for a simple Prandtl-type, laminar boundary layer, the pressure p will be approximately constant in the near wall region while the Bernoulli pressure $P = p + 1/2|\mathbf{u}|^2$ will share the $O(Re^{-1/2})$ boundary layer of the velocity field.

Point 3 is possibly related to aliasing errors; interestingly, the aliasing error in using different forms of the nonlinearity is governed by the resolution of the (Bernoulli or kinematic) pressure. Our suggestion of a "fix" of using *grad–div* stabilization (see Section 2.3) works in our tests because it addresses point 3 without requiring extra resolution.

Stabilization of *grad–div* type reduces the error in div$\mathbf{u}^h$, see (2.15), and its (bad) scaling with respect to the Reynolds number. Moreover, since when div$\mathbf{u}^h = 0$ the nonlinear terms are equivalent, this stabilization causes the three schemes to produce more closely related solutions.

Generally speaking, adding the *grad–div* terms to the finite element formulation is not a new idea. These terms are part of the streamline-upwinding Petrov–Galerkin method (SUPG) in [8,12,31]. However, in practice these terms are often omitted, and until recently it was not clear if they are needed for technical reasons of the analysis of SUPG type methods only or play an important role in computations. The role of the *grad–div* stabilization was again emphasized in the recent studies of the (stabilized) finite element methods for incompressible flow problems, see e.g. [2,3,22,23,25], also in conjunction with the rotation form, see [21,26].

We shall thus compare FEM (or other variational) discretizations of the rotation form of the NSE, given by

$$\mathbf{u}_t - \mathbf{u} \times \omega + \nabla P - v\Delta\mathbf{u} = \mathbf{f}, \qquad (1.1)$$
$$\text{div}\,\mathbf{u} = 0 \qquad (1.2)$$

with the usual convection form, given by:

$$\mathbf{u}_t + \mathbf{u} \cdot \nabla\mathbf{u} + \nabla p - v\Delta\mathbf{u} = \mathbf{f}, \qquad (1.3)$$
$$\text{div}\,\mathbf{u} = 0 \qquad (1.4)$$

and the skew-symmetric form, given by:

$$\mathbf{u}_t + \mathbf{u} \cdot \nabla\mathbf{u} + \frac{1}{2}(\text{div}\,\mathbf{u})\mathbf{u} + \nabla p - v\Delta\mathbf{u} = \mathbf{f}, \qquad (1.5)$$
$$\text{div}\,\mathbf{u} = 0. \qquad (1.6)$$

These are related by

$$P = p + \frac{1}{2}|\mathbf{u}|^2 \quad \text{and} \quad \omega = \text{curl}\,\mathbf{u}.$$

Finally, we note that the rotation and convection (or skew-symmetric) forms lead to linear algebra systems with different numerical properties, which occur in time-stepping or iterative algorithms for the NSE problem. While there is an extensive literature on solvers for the convection form, see e.g. [7], not so many results are known for the rotation form. However, the

few available demonstrate some interesting superior properties of the rotation form in this respect. In [26,28] it was shown that the rotation form enables one to take into account the skew-symmetric part of the matrix in such a way that a special pressure Schur complement preconditioner is robust with respect to all problem parameters and becomes even more effective when $v \rightarrow 0$. Such type of result is still missing for the Oseen type systems with the convective terms. An effective multigrid method for the velocity subproblem of the linearized Navier–Stokes system in the rotation form was analyzed in [27]. Finally, in [1] the special factorization of the linearized Navier–Stokes system was studied, which appears to be well suited for the rotation form.

In general, it has been reported over the years that numerical errors from a specific discretization of different forms of the nonlinear terms in the Navier–Stokes equations have different effects on the accuracy and stability of flow problems. Wilhelm and Kleiser [32] showed that for the $P_N P_{N-2}$ spectral element method (in which the velocity and pressure are approximated by polynomials of order N and $N-2$, respectively), numerical instabilities may occur in incompressible Navier–Stokes simulations when the rotational form is not used. Furthermore, they demonstrated that the reported instability is not caused by nonlinear effects, but it is rather a consequence of the staggered grid between velocity and pressure used in spectral element method. Analytical and numerical studies of incompressible Navier–Stokes equations of Kravchenko and Moin [19] show that aliasing errors are more destructive for spectral and high-order finite-difference calculations than for low-order finite-difference simulations of turbulent channel flow. The study shows that for skew-symmetric and rotational forms, both spectral and finite-difference methods are energy conserving even in the presence of aliasing errors. The effect on aliasing errors of the formulation of nonlinear terms for Burger's equations and for compressible Navier–Stokes equations was examined by Blaisdell et al. [4] using a Fourier analysis and numerical experiments. The skew-symmetric form of the convective term is the form that reduced amplitude of the aliasing errors as shown theoretically and experimentally. The analysis method for the rotational form was too complicated to draw any conclusions regarding it. Alternative forms of the compressible Navier–Stokes equations were also studied from the heuristic point of view by Kennedy and Gruber [18]. Finally, we note that the name "rotation form" is sometimes attributed to the sum of *two* terms: $(\nabla \times \mathbf{u}) \times \mathbf{u} + \frac{1}{2}\nabla|\mathbf{u}|^2$ [14,15,32], while in this paper we treat $\frac{1}{2}|\mathbf{u}|^2$ as a part of the Bernoulli pressure variable. Due to typically different discretizations (meshes) for pressure and velocity, these two alternatives lead to discrete problems with different properties. Thus, if $\frac{1}{2}|\mathbf{u}|^2$ is treated as a part of the pressure term, we expect that the under resolution of Bernoulli pressure variable may affect not only finite element, but other type of discretizations as well.

2. Differences between the nonlinearities

We now illustrate some differences between the three different forms of the NSE nonlinearity. First we discuss the Bernoulli pressure, which is used instead of usual pressure, with the rotation form of the nonlinearity, and present a bound (based on the velocity part of the Bernoulli pressure) for the rotation form FEM residual in the convective form FEM. Next, we elaborate the difference in conservation laws of the (FEM discretized) nonlinearities. Lastly in this section, we present a brief description of *grad–div* stabilization, discuss how it reduces the differences between the nonlinearities, and show how its use allows for better scaling of velocity error with the Reynolds number.

2.1. Rotation form and Bernoulli pressure

The resolution of the Bernoulli pressure (a linear effect) also critically influences the difference between the nonlinearity in the convective and rotation forms. We show that it depends upon the resolution of (the zero mean part of) the kinetic energy in the pressure space. This is the dominant part of the Bernoulli pressure. To quantify this dependence, consider the rotation-form-FEM for the simplest nonlinear (internal) flow problem, the equilibrium NSE under no-slip boundary conditions. Let U_h, Q_h denote the velocity–pressure finite element spaces. The usual $L^2(\Omega)$ inner product and norm are always denoted by $(\cdot, \cdot)$ and $\|\cdot\|$. The velocity–Bernoulli pressure approximations $\mathbf{u}_h, P_h$ satisfy

$$v(\nabla \mathbf{u}_h, \nabla \mathbf{v}_h) - (\mathbf{u}_h \times \text{curl}\,\mathbf{u}_h, \mathbf{v}_h) + (q_h, \text{div}\,\mathbf{u}_h) - (P_h, \text{div}\,\mathbf{v}_h) = (\mathbf{f}, \mathbf{v}_h) \quad (2.1)$$

for all $\mathbf{v}_h, q_h \in U_h, Q_h$. If V_h denotes the usual space of discretely divergence free velocities

$$V_h := \{\mathbf{v}_h \in U_h : (q_h, \text{div}\,\mathbf{v}_h) = 0 \ \forall q_h \in Q_h\},$$

then the approximate velocity $\mathbf{u}_h$ from (2.1) satisfies

$$v(\nabla \mathbf{u}_h, \nabla \mathbf{v}_h) - (\mathbf{u}_h \times \text{curl}\,\mathbf{u}_h, \mathbf{v}_h) = (\mathbf{f}, \mathbf{v}_h) \quad \forall \mathbf{v}_h \in V_h. \quad (2.2)$$

Similarly, the FEM formulation for the convective form formulation is given by

$$v(\nabla \mathbf{u}_h, \nabla \mathbf{v}_h) + (\mathbf{u}_h \cdot \nabla \mathbf{u}_h, \mathbf{v}_h) = (\mathbf{f}, \mathbf{v}_h) \quad \forall \mathbf{v}_h \in V_h. \quad (2.3)$$

The natural measure of the distance of the rotation forms approximate velocity from satisfying the convective forms discrete equations is the norm of residual of the former in the latter. Define this residual $\mathbf{r}_h \in V_h$ via the Riesz representation theorem as usual by

$$(\mathbf{r}_h, \mathbf{v}_h) := (\mathbf{f}, \mathbf{v}_h) - [v(\nabla \mathbf{u}_h, \nabla \mathbf{v}_h) + (\mathbf{u}_h \cdot \nabla \mathbf{u}_h, \mathbf{v}_h)] \quad \forall \mathbf{v}_h \in V_h. \quad (2.4)$$

Proposition 1. *Let $\mathbf{u}_h$ be the solution of (2.1) and let $\mathbf{r}_h$ be its residual in (2.3), defined by (2.4) above. Let*

$$M = \text{mean}\left(\frac{1}{2}|\mathbf{u}_h|^2\right) = \frac{1}{|\Omega|}\int_\Omega \frac{1}{2}|\mathbf{u}_h|^2 \mathrm{d}x.$$

Then,

$$\|\mathbf{r}_h\|_{(V_h)'} \leqslant \sup_{\mathbf{v}\in V_h, \text{div}\,\mathbf{v}_h \neq 0} \frac{(\mathbf{r}_h, \mathbf{v}_h)}{\|\nabla \cdot \mathbf{v}_h\|} \leqslant \inf_{q_h \in Q_h}\left\|\left[\frac{1}{2}|\mathbf{u}_h|^2 - M\right] - q_h\right\|.$$

Proof. Using the vector identity $-\mathbf{u}_h \times \text{curl}\,\mathbf{u}_h + \nabla(\frac{1}{2}|\mathbf{u}_h|^2) = \mathbf{u}_h \cdot \nabla \mathbf{u}_h$ gives that, for any real number M, (and in particular for $M = \text{mean}(\frac{1}{2}|\mathbf{u}_h|^2)$),

$$(\mathbf{r}_h, \mathbf{v}_h) = -\left(\nabla\left(\frac{1}{2}|\mathbf{u}_h|^2 - M\right), \mathbf{v}_h\right) = \left(\left[\frac{1}{2}|\mathbf{u}_h|^2 - M\right] - q_h, \nabla \cdot \mathbf{v}_h\right) \quad \forall q_h \in Q_h.$$

(We have integrated by parts and used $(q_h, \text{div}\,\mathbf{v}_h) = 0, \forall q_h \in Q_h$.) The Cauchy–Schwarz inequality and duality implies that, as claimed,

$$\sup_{\mathbf{v}\in V_h, \text{div}\,\mathbf{v}_h \neq 0} \frac{(\mathbf{r}_h, \mathbf{v}_h)}{\|\nabla \cdot \mathbf{v}_h\|} \leqslant \inf_{q_h \in Q_h}\left\|\left[\frac{1}{2}|\mathbf{u}_h|^2 - M\right] - q_h\right\|. \qquad \square$$

2.2. Conservation properties of the nonlinearities

The conservation properties of an algorithm can provide insight into both the physical fidelity and accuracy of its solutions. Fundamental quantities of the NSE such as energy ($E = \frac{1}{2}\|\mathbf{u}\|^2$), helicity ($H = (\mathbf{u}, \nabla \times \mathbf{u})$), and in 2d enstrophy ($Ens = \frac{1}{2}\|\nabla \times \mathbf{u}\|$), play critical roles in the organization of a flow's structures. The NSE holds delicate physical balances for each of these quantities, and these balances reveal how each term of the NSE contributes to their development. An NSE algorithm enforcing similar balances (e.g. discrete analogs) for energy, and helicity or 2d enstrophy is thus more likely to admit solutions with similar physical characteristics as the true solution.

To gain insight into the balances admitted by an algorithm, conservation laws are typically studied in the periodic case without external or viscous forces. Although this case is of little practical interest, if an algorithm fails to uphold conservation in this flow setting, it has little hope for predicting correct physical balances in irregular domains and/or complex boundary conditions.

Consider now conservation laws for energy and helicity in Crank–Nicolson FEM schemes for the NSE with rotation form (1.1) and (1.2), convective form (1.3) and (1.4), and skew-symmetric form (1.5) and (1.6). The schemes are defined by: given $\mathbf{u}_h^0 \in V_h, \mathbf{f} \in L^2(0, T; V_h')$, time step $\Delta t > 0$, kinematic viscosity $v > 0$, end time T, find $\mathbf{u}_h^i \in V_h$ for $i = 1, 2, \ldots, \frac{T}{\Delta t}$ satisfying rotation form:

$$\frac{1}{\Delta t}\left(\mathbf{u}_h^{n+1} - \mathbf{u}_h^n, \mathbf{v}_h\right) + b_r\left(\mathbf{u}_h^{n+\frac{1}{2}}, \mathbf{u}_h^{n+\frac{1}{2}}, \mathbf{v}_h\right) + v\left(\nabla \mathbf{u}_h^{n+\frac{1}{2}}, \nabla \mathbf{v}_h\right) = \left(\mathbf{f}^{n+\frac{1}{2}}, \mathbf{v}_h\right) \quad \forall \mathbf{v}_h \in V_h. \tag{2.5}$$

Convective form:

$$\frac{1}{\Delta t}\left(\mathbf{u}_h^{n+1} - \mathbf{u}_h^n, \mathbf{v}_h\right) + b_c\left(\mathbf{u}_h^{n+\frac{1}{2}}, \mathbf{u}_h^{n+\frac{1}{2}}, \mathbf{v}_h\right) + v\left(\nabla \mathbf{u}_h^{n+\frac{1}{2}}, \nabla \mathbf{v}_h\right) = \left(\mathbf{f}^{n+\frac{1}{2}}, \mathbf{v}_h\right) \quad \forall \mathbf{v}_h \in V_h. \tag{2.6}$$

Skew-symmetric:

$$\frac{1}{\Delta t}\left(\mathbf{u}_h^{n+1} - \mathbf{u}_h^n, \mathbf{v}_h\right) + b_s\left(\mathbf{u}_h^{n+\frac{1}{2}}, \mathbf{u}_h^{n+\frac{1}{2}}, \mathbf{v}_h\right) + v\left(\nabla \mathbf{u}_h^{n+\frac{1}{2}}, \nabla \mathbf{v}_h\right) = \left(\mathbf{f}^{n+\frac{1}{2}}, \mathbf{v}_h\right) \quad \forall \mathbf{v}_h \in V_h, \tag{2.7}$$

where

$$b_r\left(\mathbf{u}_h^{n+\frac{1}{2}}, \mathbf{u}_h^{n+\frac{1}{2}}, \mathbf{v}_h\right) = -\left(\mathbf{u}_h^{n+\frac{1}{2}} \times (\text{curl}\,\mathbf{u}_h^{n+\frac{1}{2}}), \mathbf{v}_h\right),$$

$$b_c\left(\mathbf{u}_h^{n+\frac{1}{2}}, \mathbf{u}_h^{n+\frac{1}{2}}, \mathbf{w}\right) = \left(\mathbf{u}_h^{n+\frac{1}{2}} \cdot \nabla \mathbf{u}_h^{n+\frac{1}{2}}, \mathbf{v}_h\right),$$

$$b_s\left(\mathbf{u}_h^{n+\frac{1}{2}}, \mathbf{u}_h^{n+\frac{1}{2}}, \mathbf{w}\right) = \left(\mathbf{u}_h^{n+\frac{1}{2}} \cdot \nabla \mathbf{u}_h^{n+\frac{1}{2}} + \frac{1}{2}(\text{div}\,\mathbf{u}_h^{n+\frac{1}{2}})\mathbf{u}_h^{n+\frac{1}{2}}, \mathbf{v}_h\right).$$

By choosing $\mathbf{v}_h = \mathbf{u}_h^{n+\frac{1}{2}}$ in each scheme and eliminating viscous and external forces, it is revealed that $\|\mathbf{u}_h^{n+1}\|^2 = \|\mathbf{u}_h^n\|^2$ and thus energy is conserved in the rotation (2.5) and skew-symmetric (2.7) schemes. For the convective form, however, we do not have exact energy conservation. Instead (using $(q_h, \nabla \cdot \mathbf{u}_h^{n+\frac{1}{2}}) = 0$ in the last step)

Table 1
Relative flux errors at $Re = 1$.

	Number of degrees of freedom		
	338	1028	3853
Convective form	$6.24593 \cdot 10^{-8}$	$6.24593 \cdot 10^{-8}$	$6.24593 \cdot 10^{-8}$
Skew-symmetric form	$4.92659 \cdot 10^{-7}$	$6.2396 \cdot 10^{-8}$	$6.24593 \cdot 10^{-8}$
Rotation form	$1.04348 \cdot 10^{-7}$	$6.42264 \cdot 10^{-8}$	$6.25398 \cdot 10^{-8}$

$$\frac{1}{2}\|\mathbf{u}_h^{n+1}\|^2 = \frac{1}{2}\|\mathbf{u}_h^n\|^2 + \Delta t(\mathbf{u}_h^{n+\frac{1}{2}} \cdot \nabla \mathbf{u}_h^{n+\frac{1}{2}}, \mathbf{u}_h^{n+\frac{1}{2}}) = \frac{1}{2}\|\mathbf{u}_h^n\|^2 + \Delta t\left(\frac{1}{2}(\mathbf{u}_h^{n+\frac{1}{2}})^2, \nabla \cdot \mathbf{u}_h^{n+\frac{1}{2}}\right), \tag{2.8}$$

$$= \frac{1}{2}\|\mathbf{u}_h^n\|^2 + \Delta t \inf_{q_h \in Q_h}\left(\left[\frac{1}{2}(\mathbf{u}_h^{n+\frac{1}{2}})^2 - M\right] - q_h, \nabla \cdot \mathbf{u}_h^{n+\frac{1}{2}}\right), \tag{2.9}$$

$$\text{where} \quad M = \text{mean}\left(\frac{1}{2}|\mathbf{u}_h^{n+\frac{1}{2}}|^2\right) = \frac{1}{|\Omega|}\int_\Omega \frac{1}{2}|\mathbf{u}_h^{n+\frac{1}{2}}|^2 \, \mathrm{d}x. \tag{2.10}$$

Exact energy conservation in the convective form scheme (2.6) thus depends on $\mathrm{div}\,\mathbf{u}_h^{n+\frac{1}{2}}$ (and the resolution of the key component of the Bernoulli pressure in the pressure space), which is nonzero since incompressibility is only weakly enforced. Hence it is possible (and well known to be likely) that these "small" errors in the energy balance at each time step can accumulate and significantly alter the solution.

Regarding helicity (3d) and enstrophy (2d) conservation, by choosing $\mathbf{v}_h = P_{V_h}(\mathrm{curl}\,\mathbf{u}_h)$ in the three schemes, it can be seen that none of the schemes conserve helicity; indeed all of the three nonlinearities alters helicity. However, it was shown in [29] that if the curl in the rotation form nonlinearity is replaced with the V_h-projected curl, then the rotation scheme will conserve helicity. To our knowledge, no such alterations can be made to (2.6) or (2.7) to maintain physical treatment of helicity. It is pointed out in [14] that for finite-difference schemes, the rotation form shows superior conservation properties to the convective form in that rotation form conserves mean momentum, energy, helicity, enstrophy and vorticity vs. just mean momentum and energy for the convective form.

2.3. Grad–div stabilization

The three forms of the nonlinearity, and thus the three schemes (2.5)–(2.7) are equivalent when $\mathrm{div}\,\mathbf{u}_h = 0$. Since this condition is only weakly enforced, $\mathrm{div}\,\mathbf{u}_h$ may grow large enough to cause significant differences between the schemes; as our numerical experiments show, this is especially true near boundaries for the rotation form. *Grad–div* stabilization can help to correct this error for steady, incompressible flow [26], and through our experiments in Sections 3.2 and 3.4 we show that this stabilization technique is also effective for unsteady flow.

To understand better the role of adding the *grad–div* term to the finite element formulation we consider the model case of the Stokes problem:

$$-\nu\Delta\mathbf{u} + \nabla p = \mathbf{f}, \quad \text{and} \quad \mathrm{div}\,\mathbf{u} = 0 \quad \text{in } \Omega,$$
$$\mathbf{u} = 0 \quad \text{on } \partial\Omega. \tag{2.11}$$

Given normal velocity–pressure finite element spaces U_h, Q_h, satisfying the discrete inf–sup condition, the *grad–div* stabilized FEM for this problem is: Pick stabilization parameter $\gamma \geqslant 0$ and find $\mathbf{u}_h, p_h \in U_h, Q_h$ satisfying

$$\nu(\nabla\mathbf{u}_h, \nabla\mathbf{v}_h) + \gamma(\mathrm{div}\,\mathbf{u}_h, \mathrm{div}\,\mathbf{v}_h) - (p_h, \mathrm{div}\,\mathbf{v}_h) + (q_h, \mathrm{div}\,\mathbf{u}_h) = (\mathbf{f}, \mathbf{v}_h) \quad \forall\mathbf{v}_h, q_h \in U_h, Q_h. \tag{2.12}$$

For the case $\gamma = 0$ a common argument is to rescale the equations by $\tilde{p} = \nu^{-1}p, \tilde{f} = \nu^{-1}f$. This leads to a parameter-independent Stokes problem with a new pressure variable and right-hand side. One can then use known results for this Stokes problem (in $\{\mathbf{u}, \tilde{p}\}$) and transform back to the $\{\mathbf{u}, p\}$ variables. The first and most basic result in the numerical analysis of the (parameter-independent) rescaled Stokes problem is that

$$\|\nabla(\mathbf{u} - \mathbf{u}_h)\| \leqslant C\left(\inf_{\mathbf{v}_h \in U_h}\|\nabla(\mathbf{u} - \mathbf{v}_h)\| + \inf_{q_h \in Q_h}\|\tilde{p} - q_h\|\right).$$

Converting back to the original dependent variables gives

$$\|\nabla(\mathbf{u} - \mathbf{u}_h)\| \leqslant C\left(\inf_{\mathbf{v}_h \in U_h}\|\nabla(\mathbf{u} - \mathbf{v}_h)\| + \frac{1}{\nu}\inf_{q_h \in Q_h}\|p - q_h\|\right). \tag{2.13}$$

This has the interpretation that: *Velocity Error* $\sim Re \cdot$ *Pressure Error*. For example, a further development of these estimates give the error bound in the rescaled variables

$$\|\nabla(\mathbf{u} - \mathbf{u}_h)\| + \|\tilde{p} - \tilde{p}_h\| \leqslant Ch(\|\nabla\nabla\mathbf{u}\| + \|\nabla\tilde{p}\|).$$

In the original variables this immediately yields

$$\|\nabla(\mathbf{u} - \mathbf{u}_h)\| + \frac{1}{\nu}\|p - p_h\| \leqslant Ch\left(\|\nabla\nabla\mathbf{u}\| + \frac{1}{\nu}\|\nabla p\|\right) \tag{2.14}$$

with a constant C that is independent of ν. Numerical experiments, see [25], shows that (2.14) is sharp. If $\gamma > 0$, (2.12) cannot be so rescaled unless $\gamma = \nu$. Otherwise, for (2.12) the following estimate is valid [25, Theorems 4.2 and 4.3]:

Table 2
Velocity and pressure errors for NSE in test 1: various forms and Reynolds numbers.

| Reynolds number	$\|\mathbf{u} - \mathbf{u}^h\|_{\infty,0}$	$\|\nabla\mathbf{u} - \nabla\mathbf{u}^h\|_{2,0}$	$\|p - p^h\|_{\infty,0}$	$\|\nabla p - \nabla p^h\|_{2,0}$
Convective form				
1	$1.27984 \cdot 10^{-11}$	$4.0987 \cdot 10^{-11}$	$3.48078 \cdot 10^{-9}$	$2.02411 \cdot 10^{-10}$
10	$1.2750 \cdot 10^{-11}$	$4.22028 \cdot 10^{-11}$	$3.17668 \cdot 10^{-9}$	$1.26608 \cdot 10^{-10}$
Skew-symmetric form				
1	$6.56789 \cdot 10^{-5}$	$6.42861 \cdot 10^{-4}$	$1.0656 \cdot 10^{-2}$	$4.84275 \cdot 10^{-3}$
10	$8.42768 \cdot 10^{-2}$	$7.99285 \cdot 10^{-1}$	$9.18175 \cdot 10^{-1}$	$7.86798 \cdot 10^{-1}$
			$\|P - P^h\|_{\infty,0}$	$\|\|\nabla P - \nabla P^h\|\|_{2,0}$
Rotation form				
1	$1.17773 \cdot 10^{-5}$	$2.14543 \cdot 10^{-4}$	$8.35095 \cdot 10^{-3}$	$1.26205 \cdot 10^{-2}$
10	$7.42883 \cdot 10^{-3}$	$2.10991 \cdot 10^{-1}$	$8.3435 \cdot 10^{-1}$	1.26174

Table 3
Velocity and pressure errors for NSE in test 2: various forms and Reynolds numbers.

Reynolds number	$\|\mathbf{u} - \mathbf{u}^h\|_{\infty,0}$	$\|\nabla\mathbf{u} - \nabla\mathbf{u}^h\|_{2,0}$	$\|p - p^h\|_{\infty,0}$	$\|\nabla p - \nabla p^h\|_{2,0}$
Convective form				
1	$6.51439 \cdot 10^{-5}$	$6.66111 \cdot 10^{-4}$	$1.06432 \cdot 10^{-2}$	$1.34122 \cdot 10^{-2}$
10	$4.50658 \cdot 10^{-2}$	$4.76032 \cdot 10^{-1}$	$8.92802 \cdot 10^{-1}$	1.3361
Skew-symmetric form				
1	$1.19698 \cdot 10^{-5}$	$2.18059 \cdot 10^{-4}$	$3.71786 \cdot 10^{-4}$	$1.2624 \cdot 10^{-2}$
10	$7.65648 \cdot 10^{-3}$	$2.15944 \cdot 10^{-1}$	$3.90984 \cdot 10^{-2}$	1.26198
			$\|P - P^h\|_{\infty,0}$	$\|\nabla P - \nabla P^h\|_{2,0}$
Rotation form				
1	$3.19832 \cdot 10^{-12}$	$1.05429 \cdot 10^{-11}$	$9.36552 \cdot 10^{-6}$	$5.77438 \cdot 10^{-11}$
10	$3.19792 \cdot 10^{-12}$	$1.08799 \cdot 10^{-11}$	$9.35505 \cdot 10^{-5}$	$3.40516 \cdot 10^{-11}$
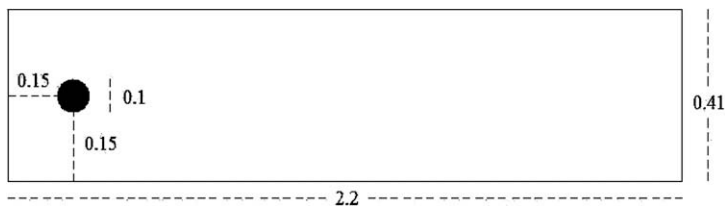
Fig. 1. Cylinder domain.
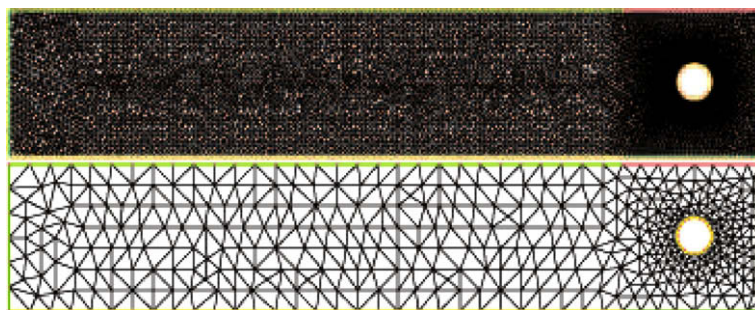
Fig. 2. Shown above are two levels of mesh refinement provided by Freefem for computing flow around a cylinder. The meshes provide, respectively, 14,455, and 56,702 degrees of freedom for the computations.

$$v^{\frac{1}{2}}\|\nabla(\mathbf{u}-\mathbf{u}_h)\| + \gamma^{\frac{1}{2}}\|\mathrm{div}(\mathbf{u}-\mathbf{u}_h)\| + \|p-p_h\| \leqslant Ch((v^{\frac{1}{2}}+\gamma^{\frac{1}{2}})\|\nabla\nabla\mathbf{u}\| + \|\nabla p\|) \tag{2.15}$$

with a constant C that is independent of v and γ. Estimates (2.14) and (2.15) suggest that for small enough v we have

$$\text{for } \gamma = 0: \quad \|\nabla(\mathbf{u}-\mathbf{u}_h)\| \simeq h\left(\|\nabla\nabla\mathbf{u}\| + \frac{1}{v}\|\nabla p\|\right),$$

$$\text{for } \gamma = 1: \quad \|\nabla(\mathbf{u}-\mathbf{u}_h)\| \simeq \frac{h}{\sqrt{v}}(\|\nabla\nabla\mathbf{u}\| + \|\nabla p\|).$$

Thus, large pressure gradients compared to the velocity second derivatives may lead to a poor convergence of the finite element velocity if one does not include *grad–div* stabilization. Otherwise, the dependence of $\|\nabla(\mathbf{u}-\mathbf{u}_h)\|$ on v is much milder.
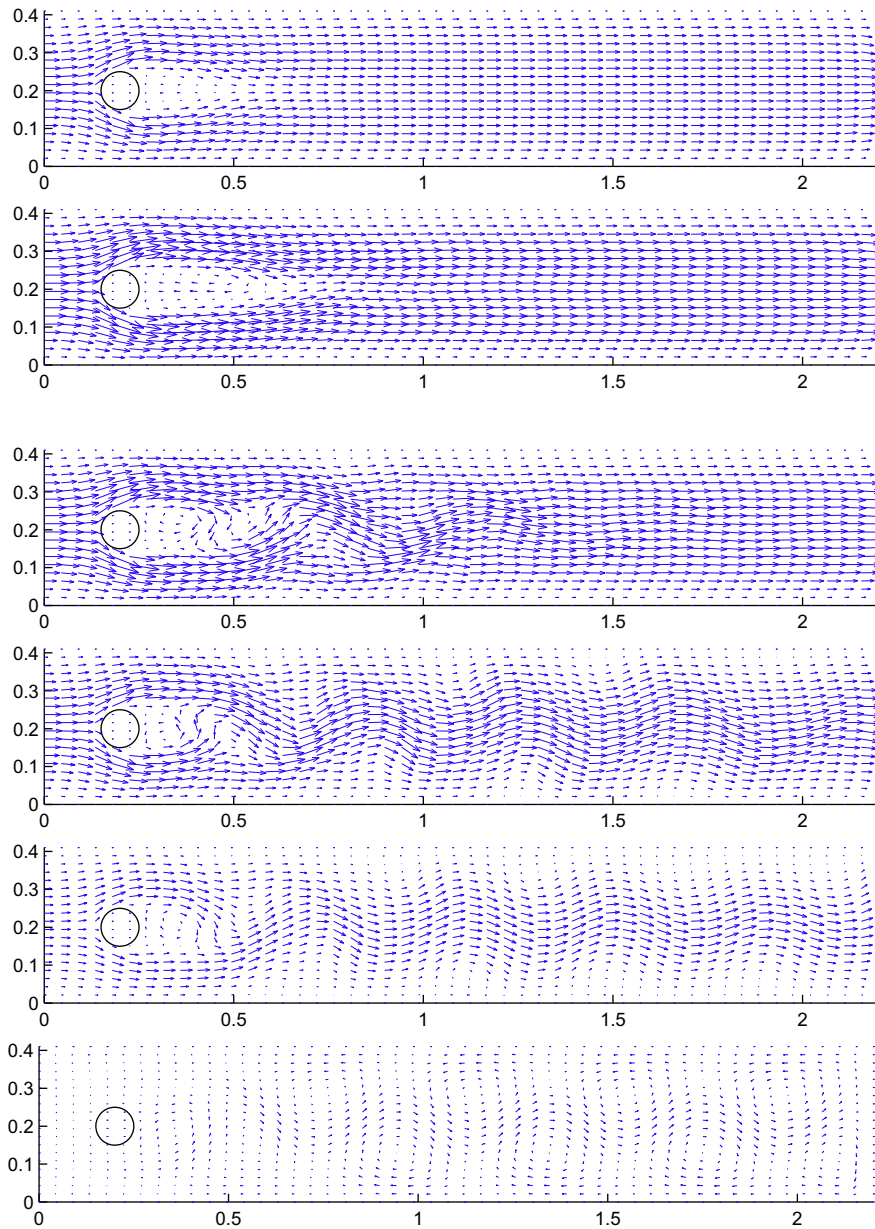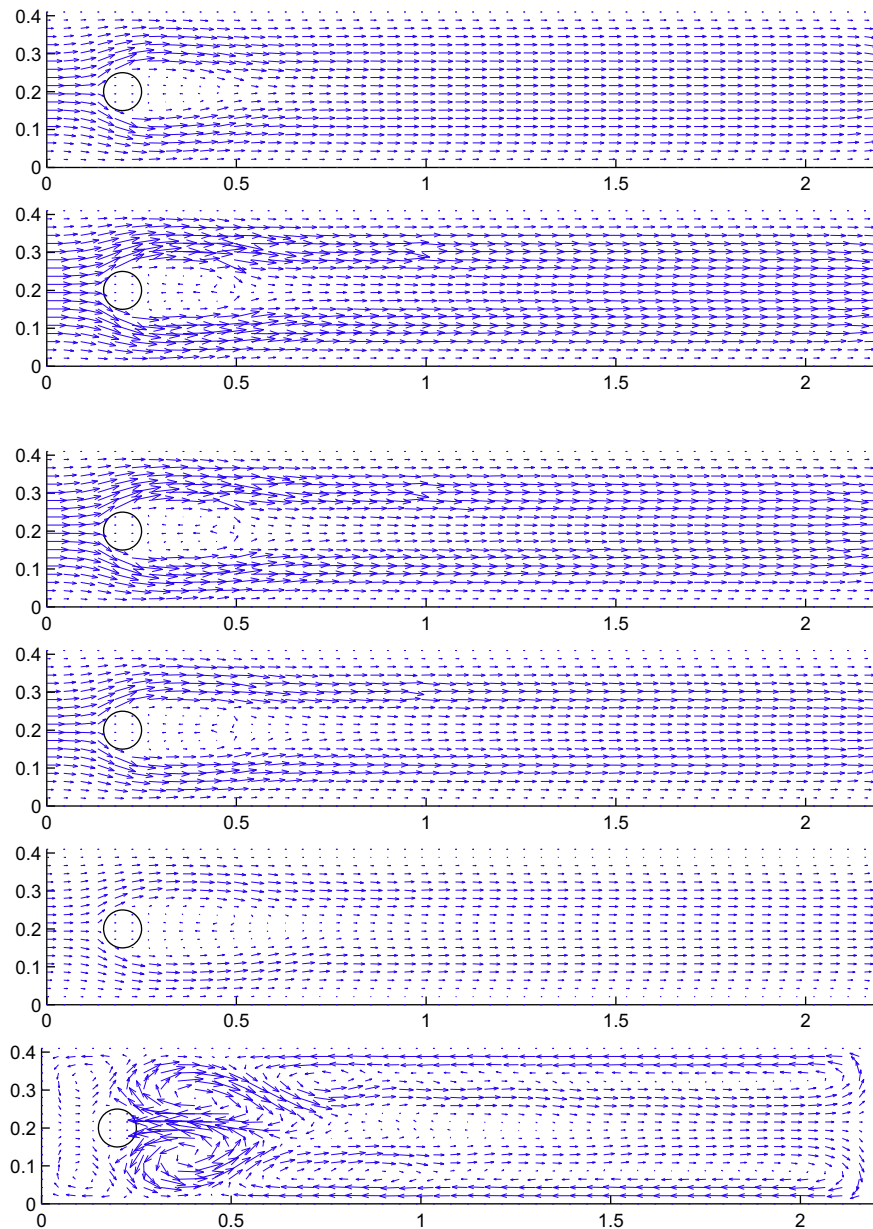

Fig. 3. Shown above is the velocity field at times $t = 2,3,5$–8 for the NSE solved on mesh 1 with the skew-symmetric form of the nonlinearity. The vortex street forms successfully.

3. Three numerical experiments

We consider three carefully chosen examples that, we believe, give strong support for the scenario of accuracy loss described in the introduction. We use the software *FreeFem++* [13] to run the numerical tests. The models are discretized with the Crank–Nicolson method in time and with the Taylor–Hood finite elements (continuous piecewise quadratic polynomials for the velocity and linears for the pressure) in space; the nonlinear system is solved by a fixed point iteration.

3.1. Test 1: Poiseuille flow

In $\Omega = (0,4) \times (0,1)$, a parabolic inflow $v(x,y,t) = 0$ and $u(x,y,t) = \frac{1}{2v}y(1-y)$ (at $x = 0$) is prescribed. No-slip boundary conditions are given at the top and bottom, and the do-nothing boundary condition is prescribed at the outflow. The exact solution is well known to be $v(x,y) = 0, u(x,y) = \frac{1}{2v}y(1-y), p(x,y) = -x + 4$, and we take it as our initial condition. A discussion

Fig. 4. Shown above is the velocity field at times $t = 2,3,5–8$ for the NSE solved on mesh 1 with the rotation form of the nonlinearity. The vortex street fails to form.

of this problem can be found in Canuto et al. [6]. The key conserved quantity in the flow is the flux through any cross section given by

$$Q(x) = \int_{0 < y < 1} u(x, y)dy = \frac{1}{12v}.$$

Note that $\mathbf{u} = (u, v)$ and p are in the finite element spaces so that we expect that discretization of the convective and skew-symmetric form of the NSE will have very small errors (comparable to the errors from numerical integration and solution of the linear and nonlinear systems arising). On the other hand, if the rotation form is used the exact solution is

$$v(x, y) = 0,$$

$$u(x, y) = \frac{1}{2v}y(1 - y),$$

$$P(x, y) = p(x, y) + \frac{1}{8v^2}y^2(1 - y)^2$$
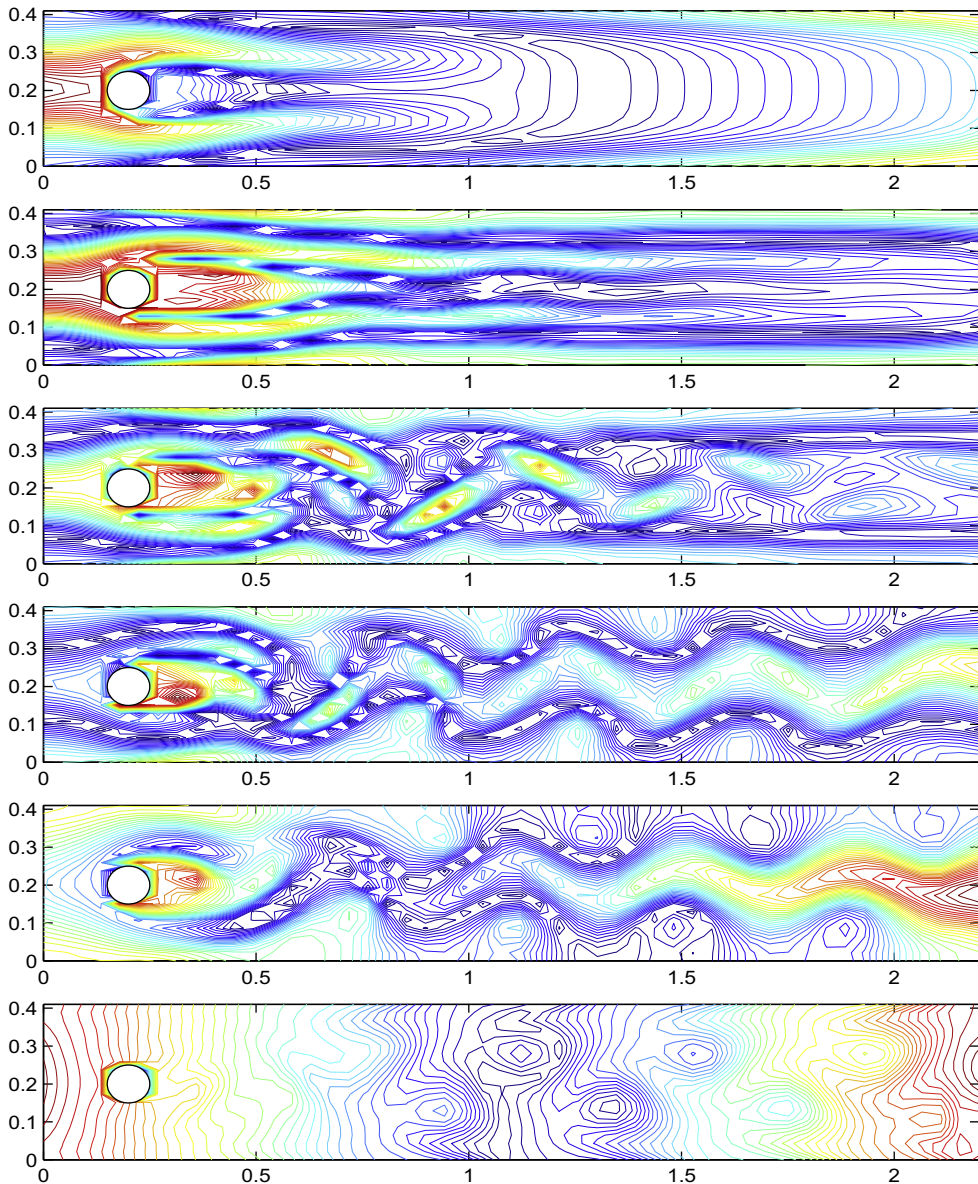

Fig. 5. Shown above is the Bernoulli pressure P at times $t = 2, 4–8$ from NSE rotation Form on mesh 2, where a vortex street forms successfully.

is not in the pressure finite element space. Thus, in the rotation form there will be discretization errors in p that influence as well the velocity error through the discrete momentum equation, since

$$P \notin Q^h \quad \text{and} \quad \|P\| = O(v^{-2}). \tag{3.1}$$

To test Poiseuille flow we take the time step $\triangle t = 0.01$ and number of time steps = 100, so the final time is $T = 1$.

For the flux computations we find that expressing the nonlinearity in different forms does not affect the true value of the flux for $Re = 1$. Results are presented in Table 1.

Next we test the coupling between velocity and pressure errors by computing the error on a fixed mesh for $Re = 1$ and $Re = 10$ (decreasing v). We present the results at the final time $T = 1$ and at the mesh level with number of degrees of freedom being 1028 in Table 2.

From Table 2, the convective form of NSE performs best with respect to the size of the velocity and pressure errors. The velocity and pressure errors for the skew-symmetric form are bigger than the corresponding errors for the convective form. It is known that skew-symmetric form of the nonlinear term of NSE imposes difficulties for simulation of Poiseuille flow [11,16], which we also observe here.
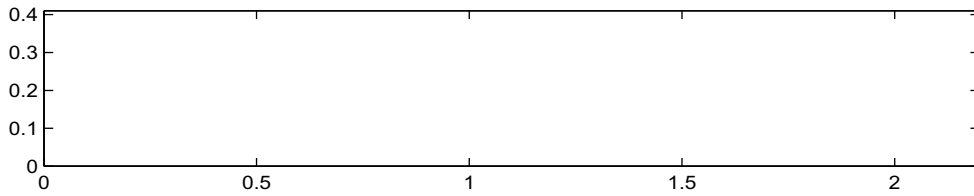
We also observe that while the velocity errors are smaller for the rotation form compared to the skew-symmetric form, the error in the (Bernoulli) pressure gradient is larger than the (usual) pressure gradient error of the skew-symmetric form. Note that for rotation form, the pressure error $\|p - p^h\|_{\infty,0}$ and the velocity error $\|\nabla(\mathbf{u} - \mathbf{u}^h)\|_{2,0}$ seem to scale like Re^3, and $\|\mathbf{u} - \mathbf{u}^h\|_{\infty,0}$ seems to scale like Re^2. Poor scaling with Re can be improved in the case of Stokes and rotation form steady NSE with the use of *grad–div* stabilization, and is our motivation in later test problems to use this stabilization.

3.2. Test 2: Resolution vs. nonlinearity

The relative importance of resolution of pressures vs. nonlinearity can be tested by artificially reversing p and P in Test 1 in a (completely) synthetic test problem. Thus, we take:

$$u(x,y) = \frac{1}{2\nu}y(1-y), \quad v(x,y) = 0, \quad P(x,y) = -x + 4,$$

so that

$$p(x,y) = -x + 4 - \frac{1}{8\nu^2}y^2(1-y)^2.$$

These are inserted in the Navier–Stokes equations to obtain a right-hand side $\mathbf{f} = \mathbf{f}(x, y, \nu)$:

$$\mathbf{f}(x, y; \nu) := \left(0, \frac{1}{4\nu^2}\left(y^2(1-y) - y(1-y)^2 \right) \right)^T.$$

The resolution of p vs. P is exactly reversed from Test 1. We present the error behavior at the final time $T = 1$ and at the mesh level with number of degrees of freedom being 1028 in Table 3.

Table 3 shows that discretization errors are present if the solution does not belong to the finite element space. The computed errors from Test 2 are the mirror image (up to the preset accuracy used for the various linear and nonlinear iterative solvers' stopping criteria) of the error behavior in the previous test. Thus it is clear that, without grad–div stabilization, in the rotation form it is the resolution of the Bernoulli pressure determine the quality of the overall velocity approximation.

3.3. Test 3: Flow around a cylinder

Next we consider the benchmark problem of flow around a circular cylinder offset slightly in a channel, from [30], see Fig. 1. The primary feature is the von Karman vortex street. To explore resolution vs. solution quality for the two formulations we test at a Reynolds number slightly above the critical one for vortex shedding and we have the simple test: *Vortex street formed yes or no.*
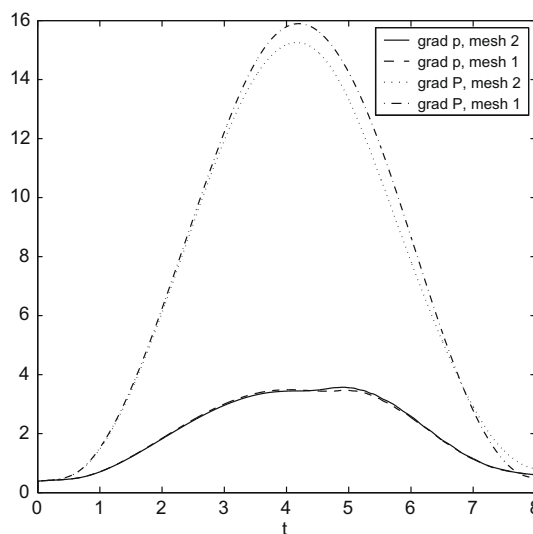

Fig. 7. Shown here is a comparison of the L^2 norm of pressure gradients from simulations of 2d flow around a cylinder on meshes 1 and 2. P denoted Bernoulli pressure from the rotation form scheme, and usual pressure from the convective form scheme is denoted by p. It is clear that ∇P is larger during the development (or lack thereof) of a vortex street.

The time dependent inflow and outflow profile are

$$u_1(0,y,t) = u_1(2.2,y,t) = \frac{6}{0.41^2} \sin(\pi t/8) y(0.41 - y),$$

$$u_2(0,y,t) = u_2(2.2,y,t) = 0.$$

No-slip boundary conditions are prescribed along the top and bottom walls and the initial condition is $\mathbf{u}(x,y,0) = \mathbf{0}$. The viscosity is set at $v = 10^{-3}$, the external force $\mathbf{f} = \mathbf{0}$, and the Reynolds number of the flow, based on the diameter of the cylinder and on the mean velocity inflow is $0 \leqslant Re \leqslant 100$. The time step is chosen to be $\Delta t = 0.005$.

Freefem generated two Delaunay meshes for testing this problem, the finest of which is able to resolve the problem for the NSE in either (rotation or skew-symmetric) form. These are shown in Fig. 2.

The velocity field calculated on mesh 1 is shown in Figs. 3 and 4. Note that

- with the skew-symmetric form the vortex street is well defined already on mesh 1 (coarse mesh);
- with the rotation form the mesh 1 simulations fails;
- with the rotation form and *grad–div* stabilization, the mesh 1 simulation forms a vortex street.
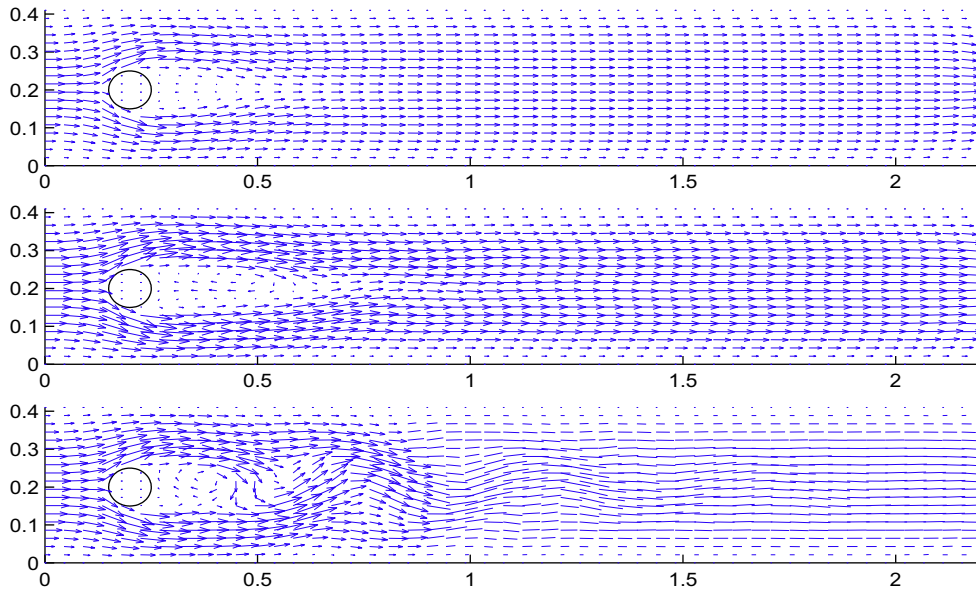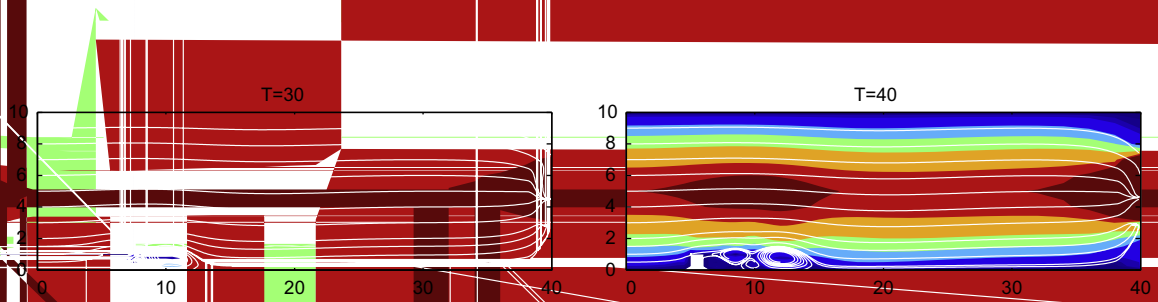
Fig. 12. NSE with *grad–div* stabilization for the rotation form.

[2] E. Burman, A. Linke, Stabilized finite element schemes for incompressible flow using Scott–Vogelius elements, Appl. Numer. Math. (2007), doi:10.1016/j.apnum.2007.11.001.
[3] M. Braack, E. Burman, V. John, G. Lube, Stabilized finite element methods for the generalized Oseen problem, Comput. Methods Appl. Mech. Eng. 196 (2007) 853–866.
[4] G.A. Blaisdell, E.T. Spryopolous, J.H. Qin, The effect of the formulation of the nonlinear terms on aliasing errors in spectral methods, Appl. Numer. Math. 21 (3) (1996) 207–219.
[5] C. Canuto, M.Y. Hussaini, A. Quarteroni, T.A. Zang, Spectral Methods in Fluid Dynamics, Springer, Berlin, 1988.
[6] C. Canuto, M.Y. Hussaini, A. Quarteroni, T.A. Zang, Spectral Methods Evolution to Complex Geometries and Applications to Fluid Dynamics, Springer, Berlin, 2007.
[7] H.C. Elman, D.J. Silvester, A.J. Wathen, Finite Elements and Fast Iterative Solvers: With Applications in Incompressible Fluid Dynamics, Numerical Mathematics and Scientific Computation, Oxford University Press, Oxford, UK, 2005.
[8] L.P. Franca, S.L. Frey, Stabilized finite element methods: II. The incompressible Navier–Stokes equations, Comput. Methods Appl. Mech. Eng. 99 (1992) 209–233.
[9] P. Gresho, R. Sani, Incompressible Flow and the Finite Element Method, vol. 2, Wiley, 2000.
[10] M.D. Gunzburger, Finite Element Methods for Viscous Incompressible Flows – A Guide to Theory, Practices, and Algorithms, Academic Press, 1989.
[11] J.G. Heywood, R. Rannacher, S. Turek, Artificial boundaries and flux and pressure conditions for the incompressible Navier–Stokes equations, Int. J. Numer. Methods Fluids 22 (1996) 325–352.
[12] P. Hansbo, A. Szepessy, A velocity–pressure streamline diffusion method for the incompressible Navier–Stokes equations, Comput. Methods Appl. Mech. Eng. 84 (1990) 175–192.
[13] F. Hecht, O. Pironneau, FreeFem++ webpage. <http://www.freefem.org>.
[14] K. Horiuti, Comparison of conservative and rotation forms in large eddy simulation of turbulent channel flow, J. Comput. Phys. 71 (1987) 343–370.
[15] K. Horiuti, T. Itami, Truncation error analysis of the rotation form of convective terms in the Navier–Stokes equations, J. Comput. Phys. 145 (1998) 671–692.
[16] V. John, Large eddy simulation of turbulent incompressible, analytical and numerical results for a class of LES models, Lecture Notes in Computational Science and Engineering, vol. 34, Springer-Verlag, Berlin, Heidelberg, New York, 2004.
[17] V. John, A. Liakos, Time dependent flow across a step: the slip with friction boundary condition, Int. J. Numer. Methods Fluids 50 (2006) 713–731.
[18] C.A. Kennedy, A. Gruber, Reduced aliasing formulations of the convective terms within the Navier–Stokes equations for a compressible fluid, J. Comput. Phys. 227 (2008) 16761700.
[19] A.G. Kravchenko, P. Moin, On the effect of numerical errors in large eddy simulations of turbulent flows, J. Comput. Phys. 131 (2) (1997) 310–322.
[20] W. Layton, C. Manica, M. Neda, L. Rebholz, Numerical analysis and computational comparisons of the NS-alpha and NS-omega regularizations, Comput. Methods Appl. Mech. Eng., in press, doi:10.1016/j.cma.2009.01.011.
[21] G. Lube, M. Olshanskii, Stable finite element calculations of incompressible flows using the rotation form of convection, IMA J. Numer. Anal. 22 (2002) 437–461.
[22] G. Matthies, G. Lube, On streamline-diffusion methods of inf–sup stable discretizations of the generalized Oseen problem, Preprint 2007-02, Institute Numerische und Angewandte Mathematik, Georg-August-Universïat Ğottingen, 2007.
[23] G. Matthies, L. Tobiska, Local projection type stabilization applied to inf–sup stable discretizations of the Oseen problem, Preprint 47/2007, Dept. Math., Otto-von-Guericke-Universitat Magdeburg, 2007.
[24] R.D. Moser, P. Moin, The effects of curvature in wall bounded flows, J. Fluid Mech. 175 (1987) 479–510.
[25] M.A. Olshanskii, A. Reusken, Grad–div stabilization for the Stokes equations, Math. Comput. 73 (2004) 1699–1718.
[26] M.A. Olshanskii, A low order Galerkin finite element method for the Navier–Stokes equations of steady incompressible flow: a stabilization issue and iterative methods, Comput. Methods Appl. Mech. Eng. 191 (2002) 5515–5536.
[27] M.A. Olshanskii, A. Reusken, Navier–Stokes equations in rotation form: a robust multigrid solver for the velocity problem, SIAM J. Sci. Comput. 23 (2002) 1682–1706.
[28] M.A. Olshanskii, Iterative solver for Oseen problem and numerical solution of incompressible Navier–Stokes equations, Numer. Linear Algebra Appl. 6 (1999) 353–378.
[29] L. Rebholz, An energy and helicity conserving finite element scheme for the Navier–Stokes equations, SIAM J. Numer. Anal. 45 (4) (2007) 1622–1638.
[30] M. Shäfer, S. Turek, Benchmark computations of laminar flow around cylinder, Flow Simulation with High-Performance Computers, vol. II, Vieweg, 1996.
[31] L. Tobiska, G. Lube, A modified streamline diffusion method for solving the stationary Navier–Stokes equations, Numer. Math. 59 (1991) 13–29.
[32] D. Wilhelm, L. Kleiser, Stable and unstable formulations of the convection operator in spectral element simulations, Appl. Numer. Math. 33 (14) (2000) 275–280.
[33] T.A. Zang, On the rotation and skew-symmetric forms for incompressible flow simulations, Appl. Numer. Math. 7 (1991) 27–40.